Structure, thermal stability and transport properties of heat-resistant high-entropy ZrTiHfNb alloy

© R.E. Ryltsev[1,2], S.Kh. Estemirova[1,2], D.A. Yagodin[1], E.V. Sterkhov[1], S.A. Uporov[1,2]

[1] Institute of Metallurgy of Ural Branch of the Russian Academy of Science,
Ekaterinburg, Russia
[2] Ural Federal University after the first President of Russia B.N. Yeltsin,
Yekaterinburg, Russia

E-mail: rrylcev@mail.ru

The problem of phase stability is one of the key problems in the study of high-entropy alloys. Here we address this issue for a heat-resistant high-entropy TiZrHfNb alloy with a bcc structure. The evolution of the structure of this alloy is studied during isothermal annealing at $T = 400°$C. It was found that the as-cast alloy consists of two coexisting bcc phases with similar unit cell parameters. This state is homogenized during annealing. Still, the highly stressed nanostructured state is retained and the texture is enhanced. The thermal conductivity of the alloy in the temperature range of $20-400°$C changes in the range of $8-16$ W/m · K, which is comparable in order of magnitude with the thermal conductivity of steels.

1. Introduction

High-entropy alloys (HEA) are multicomponent systems consisting of minimum four elements and having a composition close to equiatomic. Such alloys are characterized by four important effects: high configurational entropy, slow diffusion of elements, strong crystal lattice distortions, and „cocktail effect“ (see, for example, [1]). The study of HEA is one of the most progressive and rapidly developing areas in modern materials science, and interest in it is steadily growing.

One of the promising classes of HEA are heat-resistant HEA — alloys, including elements from the subgroups of titanium (Ti, Zr, Hf), vanadium (V, Nb, Ta) and chromium (Cr, Mo, W). Such HEA have increased chemical resistance and high mechanical strength at high temperatures [2].

The problem of stabilization of a single-phase multicomponent solid-state solution based on a certain structure has historically been a key one in this field. Currently, many multicomponent alloys of refractory elements have been synthesized and studied. Most of them are not single phase materials. As a rule, these are two-phase alloys, where the main phase is an ordered or disordered solid-state solution with a body-centered cubic structure (BCC). The second phase can be either Laves phases with a cubic (C15) or hexagonal (C14) lattice, or solid-state solutions based on hexagonal close-packed structures (HCP). There can be another structural state. For example, the authors of the work [3] synthesized a single-phase $Ti_{35}Zr_{27.5}Hf_{27.5}Nb_5Ta$ alloy with an orthorhombic structure, and in the case

of alloy $V_{35}Ti_{35}Fe_{15}Cr_{10}Zr_5$ the presence of two phases with a face-centered crystal structure (FCC) [4] was revealed.

In most cases single-phase heat-resistant HEA crystallize in BCC-structure. The following systems HfNbTaTiZr, NbTiVZr and $NbTiV_2Zr$ [5], HfNbTiZr [6], ZrNbTiVHf [7], NbReHfZrTi [8] and NbTaTiW [9] are among them. On the whole, there is a general trend: a single-phase HEA solid-state solution is stable at high temperatures (usually above 1000 K), when the configuration entropy plays a key role, but at low temperatures, the multiphase state is stable. Thus, an urgent task is to create single-phase HEA that are thermodynamically stable in the low-temperature range. For heat-resistant HEA, this is especially important in the context of the prospects for their use as materials for the needs of the nuclear industry [10]. In the article [10] it was emphasized that the operating temperature range for this application does not exceed 400°C.

In this work, we study the structure, low-temperature thermal stability, and transport properties of a single-phase heat-resistant HEA ZrTiHfNb. The existence of a single-phase solid-state solution with a BCC-structure in this system at low temperatures was first reported in [11], but the thermal stability and physical properties were not studied. Bearing in mind the results of the work [10], we limited ourselves to annealing the ZrTiHfNb alloy at $T = 400°$C, which was previously designated as the limiting temperature for use as materials for the nuclear industry [3].

2. Synthesis of the samples and measurement procedure

The initial ZrTiHfNb alloy was synthesized from elemental components with a purity of minimum 99.99% by electric arc melting in a purified helium atmosphere. To achieve homogeneity, the samples were remelted minimum 10 times, with holding in the arc at a maximum power of minimum 1 min. The phase state of the sample was controlled by X-ray diffraction analysis, as well as using an optical microscope. Since the change in the mass of the material before and after melting did not exceed 0.1 at%, it can be argued that the overall formula of the obtained alloy corresponded to the equiatomic composition of ZrTiHfNb.

The X-ray diffraction analysis of the obtained sample showed the formation of a disordered solid-state solution with a BCC-structure. The thermal analysis concluded that when this sample is heated to $400°C$, there are no thermal effects, which indicates that phase transformations do not occur in this temperature range. Next, the sample was subjected to cyclic heat treatment in the following mode: 1) heating at a rate of 5 K/min to $400°C$; 2) exposure at $T = 400°C$ for $1-3$ h; 3) cooling at a rate of 5 K/min. This cycle was repeated three times. Isothermal exposure during the first two annealings was 1 h, during the third annealing — 3 h.

At all these stages of heat treatment, the calorimetric control of the transformations occurring in the system was carried out using a Netzsch STA 449C instrument.

The phase composition and microstructural parameters of the heat-treated samples were analyzed using X-ray diffraction analysis (Shimadzu XRD-7000 diffractometer) in a single-step operation in the angular range $2\Theta = 20-120°$, $\Delta(2\Theta) = 0.03°$, exposure at point 3 sec. The analysis of the physical line broadening was carried out by the Williamson−Hall method, using an expression that takes into account the joint contribution from small CSR (coherent scattering region) and lattice distortions: $\beta = 4\varepsilon \cdot \mathrm{tg}\,\Theta + \lambda_x/(D \cdot \cos \Theta)$, where β — physical broadening (rad), ε — microdistortion value (dimensionless value), λ_x — radiation wavelength (nm), Θ — Bragg angle (rad), D — average CSR (nm).

The thermal diffusivity α was measured by the laser flash method on a Netzsch LFA 457 instrument. Heat capacity C_p was calculated using a standard comparison method with the use of Inconel 600 alloy as a reference. The thermal conductivity λ was calculated using the well-known relation $\lambda = \alpha d C_p$, where d is the density of the sample.

3. Results and discussion

X-ray diffraction analysis showed that the TiZrHfNb alloy crystallizes in a body-centered cubic structure (BCC, sp. gr. $Im-3m$) (Fig. 1). However, the Bragg reflections (200) and (311) are presented as well-resolved doublets (Fig. 1). This indicates the presence of two BCC-phases (are denoted as BCC1 and BCC2 in Fig. 1) with close interplanar spacings and different chemical compositions [12]. The heterogeneity of the chemical composition is typical during the crystallization of multicomponent alloys, when more refractory components crystallize first, and the peripheral layers and intergranular spaces are enriched with less refractory components.

The diffraction peaks of the initial sample are significantly broadened. An analysis of their width (full width at half height) by the Williamson−Hall method showed that the broadening is caused both by small CSR sizes and by the presence of rather large values of lattice microdistortions (table). The small sizes of CSR are probably the result of a high concentration of defects in the crystal structure, as well as the formation of a nanostructured state during rapid crystallization. The high intensity line (200) is the result of the texture.

After heat treatment, the structural-phase state of the alloy did not change. However, some significant points can be noted.

The most obvious process during heat treatment is the homogenization of the alloy, i.e. more complete mixing of the components and the achievement of a homogeneous state of the material. This is evidenced by the decrease in the splitting of the Bragg peaks after the second and third cycles. The annealing process should be accompanied by coarsening of crystallites (D) and removal of stresses (ε) arising during hardening after arc melting. However, this is not in our case, minimum during 5 h annealing (table). There is no tendency for these parameters (D and ε) to change depending on the annealing time. The preferred orientation of crystallites (texture) present in the original alloy even increased to such an extent that the reflections (220) and (321) disappeared already after the first hour of annealing.

Taking into account that low-temperature allotropic modifications of titanium, zirconium and hafnium have a hexagonal structure [13], it can be expected that the alloy can

Phase composition, crystal structure parameter, average size of coherent scattering areas ($\langle D \rangle$), average value of microdistortions ($\langle \varepsilon \rangle$) of TiZrHfNb alloy subjected to thermal cycling

Method of processing	Phase composition	a, nm	$\langle D \rangle$, nm	$\langle \varepsilon \rangle \cdot 10^{-3}$
Initial ingot	BCC1	0.3457 (1)	63	4.0
	BCC2	0.3438 (8)	63	3.6
$T = 400°C$ (annealing I)	BCC1	0.3450 (2)	71	6
	BCC2	0.3422 (9)	90	2.8
$T = 400°C$ (annealing II)	BCC1	0.3452 (2)	91	5
	BCC2	0.3434 (7)	37	2.4
$T = 400°C$ (annealing III)	BCC1	0.3450 (3)	46	6
	BCC2	0.3436 (7)	90	−9
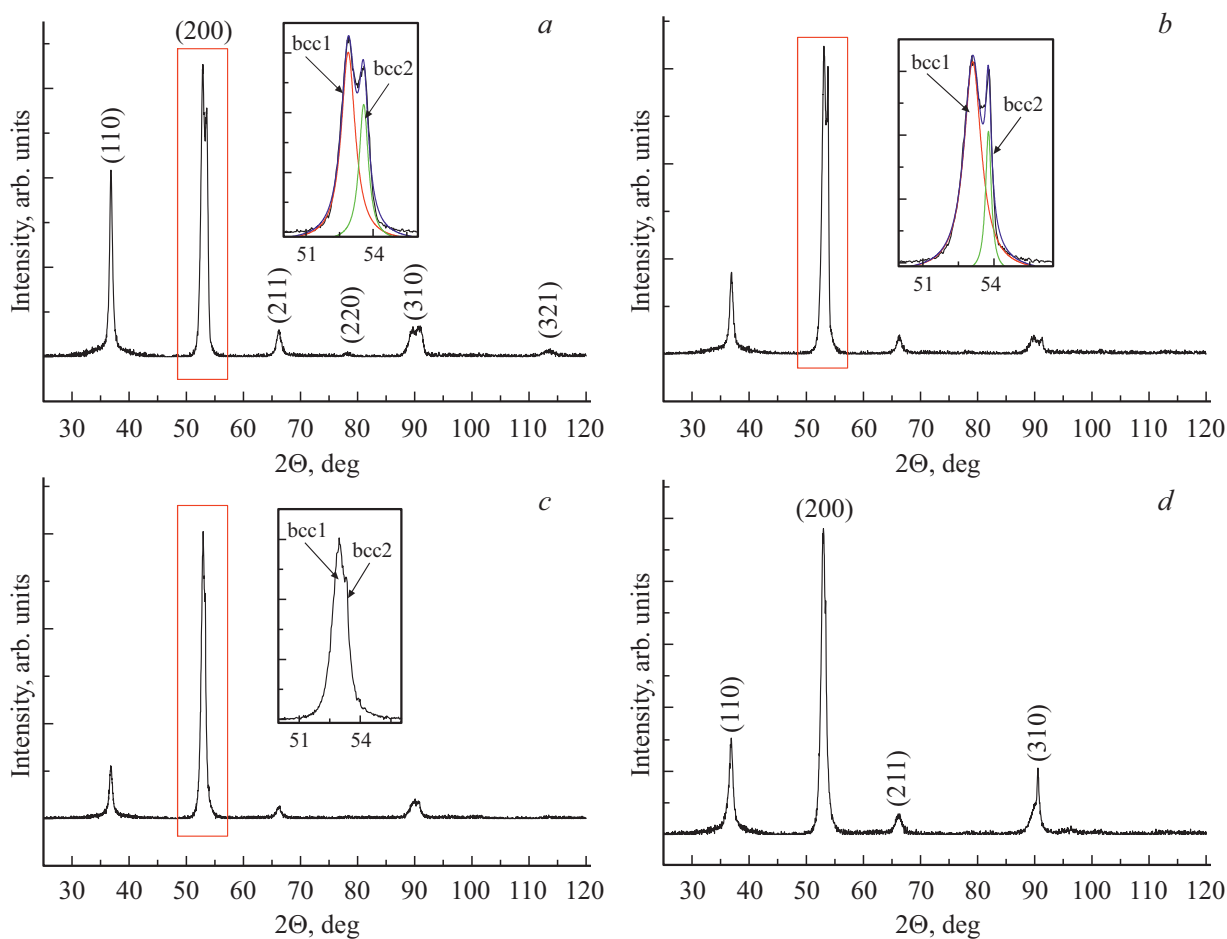
Figure 1. X-ray diffraction patterns of the original (*a*) and annealed TiZrHfNb sample at $T = 400°C$: *b, c, d* — first, second and third cycles respectively. The insets show an enlarged fragment showing the splitting of the line (200) of the BCC-structure.
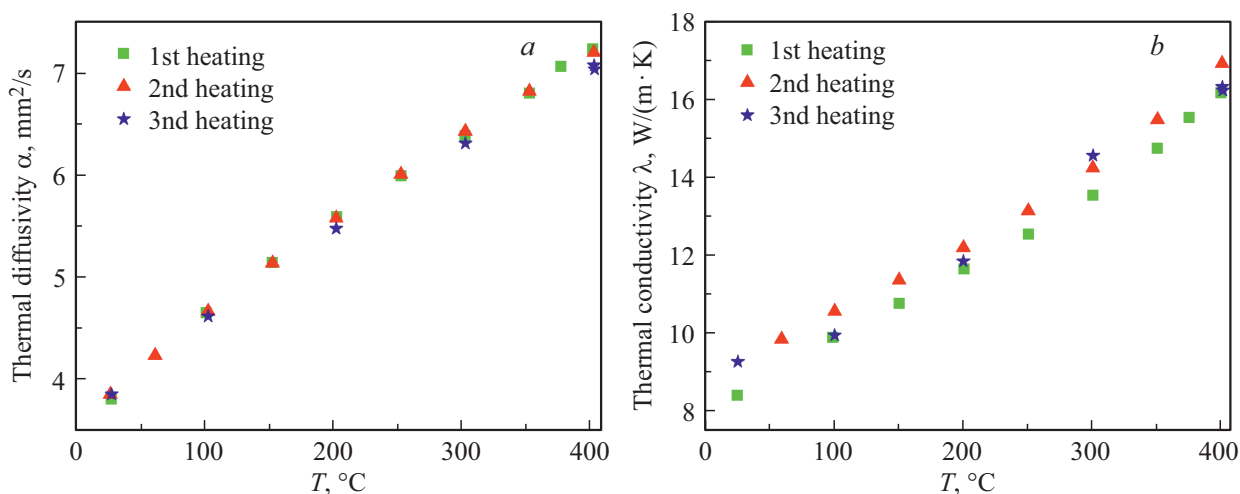
Figure 2. Temperature dependences of the thermal diffusivity (*a*) and thermal conductivity (*b*) of the TiZrHfNb alloy during successive heating cycles.

pass into a two-phase state at long times of thermal aging at low temperatures. On the other hand, the niobium present in the alloy, which crystallizes only in the BCC-structure, can stabilize the BCC-structure or, at least, slow down the

kinetics of the transition of the composition to the two-phase state. To study the conditions for achieving equilibrium of the phase state of a given alloy, a longer time may be required.

In the context of possible applications of high-temperature HEA, it is important to study their transport properties, in particular, thermal conductivity. Figure 2 shows the temperature dependences of the thermal diffusivity (α) and thermal conductivity (λ) of the TiZrHfNb alloy obtained by heating from room temperature to 400°C (before isothermal holding) successively for each heat treatment cycle.

It can be seen from Fig. 2 that the values α and λ are practically the same for all three successive heating cycles, that is, they do not change significantly in

In the course of isothermal annealings. The absolute values of these quantities are comparable with those in steels [14]. Such values are acceptable for alloys used as materials for the nuclear industry, the main requirement of which is high radiation resistance, which is the case for the alloy TiZrHfNb [10] studied by us.

4. Conclusion

The low-temperature stability of a heat-resistant high-entropy TiZrHfNb alloy with a BCC-structure at $T = 400$°C has been studied. It has been found that the heterogeneous state formed as a result of arc melting (the coexistence of two BCC-phases with a close lattice cell parameter) is homogenized during annealing. Meanwhile, the highly stressed nanostructured state is preserved and the texture is enhanced.

The thermal conductivity of the alloy in the specified temperature range varies in the range of $8-16\,\text{W/m} \cdot \text{K}$, which is comparable in order of magnitude with the thermal conductivity of steels. These properties determine the prospects for using the studied alloy as materials for the needs of the nuclear industry.

Conflict of interest

The authors declare that they have no conflict of interest.

References

[1] Y. Zhang, T.T. Zuo, Z. Tang, M.C. Gao, K.A. Dahmen, P.K. Liaw, Z.P. Lu. Prog. Mater. Sci. **61**, 1 (2014).
[2] J. Chen, X. Zhou, W. Wang, B. Liu, Y. Lv, W. Yang, D. Xua, Y. Liu. J. Alloys Comp. **760**, 15 (2018).
[3] L. Lilensten, J.P. Couzinié, L. Perriére, J. Bourgon, N. Emery, I. Guillot. Mater. Lett. **132**, 123 (2014).
[4] X. Xian, Z. Zhong, B. Zhang, K. Song, C. Chen, S. Wang, J. Cheng, Y. Wu. Mater. Des. **121**, 229 (2017).
[5] O.N. Senkov, S.V. Senkova, D.B. Miracle, C. Woodward. Mater. Sci. Eng. A **565**, 51 (2013).
[6] Y.D. Wu, Y.H. Cai, T. Wang, J.J. Si, J. Zhu, Y.D. Wang, X.D. Hui. Mater. Lett. **130**, 277 (2014).
[7] M. Feuerbacher, T. Lienig, C. Thomas. Scripta Mater. **152**, 40 (2018).
[8] S. Marik, M. Varghese, K.P. Sajilesh, D. Singh, R.P. Singh. J. Alloys Comp. **769**, 1059 (2018).
[9] F.G. Coury, T. Butler, K. Chaput, A. Saville, J. Copley, J. Foltz, P. Mason, K. Clarke, M. Kaufman, A. Clarke. Mater. Design **155**, 244 (2018).
[10] D.J.M. King, S.T.Y. Cheung, S.A. Humphry-Baker, C. Parkin, A. Couet, M.B. Cortie, G.R. Lumpkin, S.C. Middleburgh, A.J. Knowles. Acta Mater. **166**, 435 (2019).
[11] Y.D. Wu, Y.H. Cai, T. Wang, J.J. Si, J. Zhu, Y.D. Wang, X.D. Hui. Mater. Lett. **130**, 277 (2014).
[12] K.M. Youssef, A.J. Zaddach, C. Niu, D.L. Irving, C.C. Koch. Mater. Res. Lett. **3**, 95 (2015).
[13] N.P. Lyakishev. Diagrammy sostoyaniya dvojnykh metallicheskikh sistem: Spravochnik. Mashinostroenie, M. (1997). Vol. 2. 1024 p. (in Russian).
[14] S.V. Stankus, I.V. Savchenko, A.V. Baginskii, O.I. Verba, A.M. Prokop'ev, R.A. Khairulin. High Temperature **46**, 731 (2008).